Arch. Metall. Mater. **64** (2019), 4, 1321-1326

DOI: 10.24425/amm.2019.130097

K. DYBOWSKI*[#], G. ROMANIAK*, P. KULA*, A. JEZIORNA*, P. KOWALCZYK*,
R. ATRASZKIEWICZ*, Ł. KOŁODZIEJCZYK*, D. NOWAK*, P. ZAWADZKI*, M. KUCIŃSKA**

IMPACT OF THE METHOD OF SEPARATING GRAPHENE FROM THE GROWTH SUBSTRATE ON THE QUALITY OF THE 2D MATERIAL OBTAINED

This article presents the research results on impact of the method of polycrystalline graphene layers separation from the growth substrate on the obtained carbon material quality. The studies were carried out on graphene sheets obtained by metallurgical method on a liquid metal substrate (HSMG® graphene). The graphene was separated using chemical etching method or the electrochemical delamination method, by separating by means of electrolysis. During electrolysis, hydrogen is emitted on a graphene-covered of cathode (metal growth substrate) as a result of the voltage applied. The graphene layer breaks away from metallic substrate by gas accumulation between them. The results from these separation processes were evaluated by means of different tools, such as SEM, TEM and AFM microscopy as well as Raman Spectroscopy. In summary, the majority of analyses indicate that the graphene obtained as a result of hydrogen delamination possesses higher purity, smaller size and number of defects, its surface is smooth and less developed after the transfer process to the target substrate.

Keywords: graphene, polycrystalline graphene, electrochemical delamination, chemical etching, graphene transfer

1. Introduction

Graphene is a monoatomic structure composed of carbon with sp^2 hybridisation. It is characterised by high mobility of carriers, reaching up to 2.3×10^5 cm^2 V^{-1} s^{-1}, irrespective of wavelength (from THz to UV frequency) light absorbance at the level of 2.3, high theoretical strength [1], and thermal conductivity of about 4000 W m^{-1} K^{-1} [2]. The unique features of graphene referred to above made it an object of interest with regard to potential applications in e.g. high frequency transistors [3], supercapacitors [4], composites for water treatment [5], optoelectronics [1] and other applications. Graphene production methods include simple methods such as mechanical exfoliation, which was applied by Novoselov when he obtained graphene for the first time in 2004 from highly oriented pyrolytic graphite (HOPG) [6-8], chemical exfoliation [9], growth on silicon carbide [9-11], chemical sedimentation from gaseous phase (CVD) [9,11-14], or metallurgical method consisting in producing graphene on liquid copper substrate (HSMG®) elaborated at Łódź University of Technology [15-16].

After producing graphene, an important and difficult step consists in its transfer, which is indispensable for further research and practical applications. The FRePECTE method (Flattening, graphene layer Removal, polymer layer Protection, Etching, Cleaning, Transfer, polymer Elimination) is used for separating large-surface graphene [11]. Similarly to the majority of methods of this type, the main steps are graphene straightening [17], application of a protective polymer layer that also serves as temporary substrate, removal of metallic substrate and elimination of polymer after transferring graphene to the target surface [18]. Other methods include "Roll to roll" method [11] and direct transfer without presence of polymer [17]. What is dynamically developing at present is the electrochemical delamination. Similarly to the case of wet transfer, graphene is covered with polymer, submerged in aqueous solution of electrolyte and subjected to the voltage applied. The graphene on the growth substrate is polarised negatively. As a result of electrolysis, hydrogen is emitted between the metallic substrate and graphene, leading to delamination [19]. Progressive submersion of the sample leads to occurrence of hydrogen "bubbling" on one edge, which improves control over the process [20], leads to perfect "laying" of graphene on the solution and the additional mechanical force related to liquid surface tension facilitates delamination [21]. The literature mentions application of various types of electrolytes [20-25], voltages [20-23,25] and currents [23-24].

This article presents the results of qualitative studies of polycrystalline graphene layers separated from the growth surface by means of the hydrogen delamination method and the currently commonly applied method of chemical etching of the metallic substrate in iron chloride. The comparison of these two methods enables indicating qualitative differences resulting from the separation method applied.

* LODZ UNIVERSITY OF TECHNOLOGY, INSTITUTE OF MATERIALS SCIENCE AND ENGINEERING, 1/15 STEFANOWSKIEGO STR., 90-924, ŁÓDŹ, POLAND
** NANOMATERIAL STRUCTURAL RESEARCH LABORATORY, BIONANOPARK SP. Z O.O. [LTD.]
[#] Corresponding author: konrad.dybowski@p.lodz.pl

2. Material and methods

Layers of polycrystalline graphene produced using the metallurgical method on a liquid metal substrate (HSMG® graphene) [15-16] were used for the purposes of the research. The nickel substrate in the form of metal sheets with thickness of 0.15 mm and dimensions of 200×100 mm^2 was coated galvanically with copper in saturated solution of copper sulphate pentahydrate ($CuSO_4 \cdot 5H_2O$) for 6 hours with current density of 2 A dm^{-2}, providing a 0.2 mm thick layer of copper. The graphene production process was performed in a SuperCarb of the Seco/Warwick SA company, in the following stages:

(I) hot soaking in vacuum (pressure in furnace chamber =10 Pa) up to the temperature of 1060°C,
(II) carburising in carboniferous gas atmosphere (ethylene + acetylene) at the temperature of 1060°C,
(III) hot soaking up to 1110°C with an isothermal stop – time = 5 min.,
(IV) cooling together with the furnace down to the ambient temperature.

The evaluation of graphene continuity after production was carried out by performing the "oxidation test" consisting in submerging the substrate with graphene in distilled water, and then performing visual evaluation of appearance of oxidised spots on copper. Next, there was performed a "droplet test", where a droplet of the $FeCl_3$ reagent with concentration of 0.1 mol dm^{-3} was placed on the surface of graphene for 5 seconds and then rinsed with water. The effects of interaction of water and iron chloride with the surface were evaluated after a thorough analysis on a Nikon Eclipse MA200 light microscope.

Continuous graphene layer protects cooper from oxidation, therefore in the areas where graphene wasn't created or was defected, darker colouring occur. The pictures show defects in the form of longitudinal (marked as 1 in Fig. 1a) and point cracks in the created layer of graphene. Some of them got revealed after test with water. Treatment with $FeCl_3$ caused deepening of cracks and revealed more point defects (marked as 2 in Fig. 1b) with different size and density of occurrence.

Next, graphene samples with size of 10×10 mm^2 were prepared for electrochemical delamination and separation by means of chemical etching. Coating with a temporary carrier layer – a polymer – was performed by means of drop coating. PMMA with Mw ~ 996000 of the Aldrich Chemistry company, dissolved in chlorobenzene with concentration of 0.05 mol dm^{-3} (4.6 g of PMMA – 100 ml of chlorobenzene) was applied. The thickness of the layer deposited fluctuated from 10 μl cm^{-2} to 50 μl cm^{-2} of liquid polymer. Polymer drying took place in the temperature of 40°C for about 30 minutes.

Delamination was carried out at an automatic laboratory station made specially for that purpose. This station enables full automation of the separation process, including the possibility of controlling the key parameters such as voltage and current, sample inclination angle, and speed of submersion in electrolyte. The optimal parameters for delamination process, for which the best graphene quality was obtained after separation from metallic substrate were: 0.5 mol dm^{-3} NaOH solution, current and voltage parameters: U = 2.5-5 V, I = 0.1-1.5 A, sample submersion angle α = 45-60°, linear speed of submersion V = 0.01-0.03 mm s^{-1}. Graphene quality was characterised by determining the number and the size of defects by SEM microscopy (AEE mode) and electrical resistance measurement.

Separation of graphene by means of chemical etching was carried out in a 1 mol dm^{-3} solution of iron chloride (III) ($FeCl_3$) in the temperature of 50-55°C for the period of 4-12 hours with continuous mixing ensured. The polymer foil with graphene separated in this manner was then held sequentially in deionised water, 10% hydrochloric acid (HCl, 5-10 min.) – in order to remove the products of etching, and then once again in deionised water.

After delamination and etching, the HSMG® graphene on foils with PMMA was subjected to SEM examination with the use of Hitachi S 3000 N microscope with AEE detector in order to evaluate the degree of its defectiveness. The voltage that accelerated electrons during the examination was 5 kV.

In both cases, the graphene layer so prepared was transferred onto silicon (silicon wafers with 300 nm thick SiO_2 layer). Graphene was laid on a droplet of water and then, after removing the excess thereof, hot soaked in temperature of 50-80°C for 5-7 minutes until evaporation of water present between the graphene and the substrate. In order to eliminate the polymer, the samples were put into acetone vapours for 10-20 minutes, after which they were

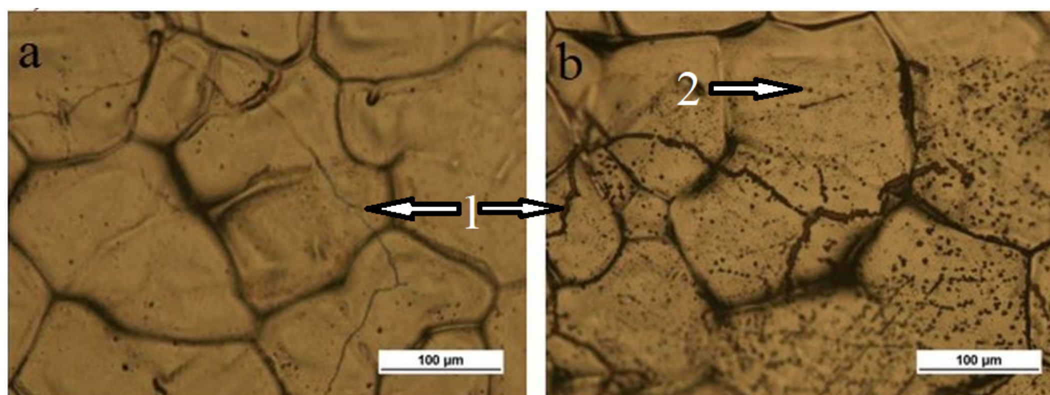

Fig. 1. Graphene on copper a) after the "oxidation test", b) after the "droplet test". 1 – linear defects, 2 – point defects. Image from the optical microscope

transferred to a cold acetone bath for about 2 hours, with the solvent being replaced twice during that time. Resistance of the layer was measured using a UNI-T UT70B multimeter with needle tipped multimeter probes in the same way for every sample on the diagonals and sides of the specimen. It was within the range of 2-6 kΩ for both separation methods. Resistance of graphene for the samples after delamination was decreasing after putting them to an exicator for several dozen hours, which may result for evaporation of residual water and/or detachment of hydrogen that became attached to the graphene surface during delamination.

After transferring onto silicon, graphene was subjected to examination by means of Multimode 5 (Bruker) atomic force microscope featuring a Nanoscope V controller. The imaging was performed in tapping mode by applying silicon probes with various geometry and spring constants of cantilever and resonance frequencies. The samples were hot soaked in the temperature of 400°C for an hour (at pressure of 2.3×10^{-3} Pa). The hot soaking was intended to cause thermal decay of presumptive remains of the polymer removed.

The analysis of graphene after transfer to silicon was performed by means of Raman spectroscope (Renishaw, GB) with laser wavelength of 532 nm. The power of the laser amounted to 10 mW. The measurements were performed at room temperature in ambient conditions.

3. Results and discussion

3.1. Microscopic evaluation of the degree of defectiveness of graphene layers after delamination

After delamination and etching, the HSMG® graphene on foils with PMMA was subjected to SEM microscope examination with use AEE detector in order to evaluate the degree of its defectiveness. The image in the AEE mode that is created during the examination results from different values of current flowing through the sample depending on whether the electron beam falls onto conductive or non-conductive areas.

Based on the SEM images of graphene on PMMA and optical image of graphene on growth substrate (Fig. 1) it can be stated that discontinuities formed in graphene at the production stage have not been intensified while separation from growth substrate. The image of the surface of a sample after delamination (Fig. 2a) shows only several linear discontinuities and projected after-effects of borders of copper grains. Growth substrate (copper) grains borders mapping is formed on PMMA, which after coating and solvent evaporation creates replica of the substrate. After graphene transfer to target substrate and PMMA elimination this effect disappears. The sample after etching (Fig. 2b) features slightly more linear discontinuities that are distributed uniformly on the whole surface area. On the basis of these observations it can be stated that delamination does not intensify these defects – their width remains at the level of a few micrometres, same as after chemical etching. On the graphene after etching there are visible more contaminations in the form of bright particles (remains of corrosion products).

3.2. Evaluation of layer continuity in nanoareas and examination of graphene surface topography by means of atomic force microscopy

After hot soaking of the graphene transferred onto silicon, it is visible already on the optical microscope preview that the purity achieved is clearly higher in case of delamination (Fig. 3a) than in case of chemical etching (Fig. 3b). The yellow stains visible on the sample after etching do not constitute residue of the polymer as it would undergo degradation in such a high temperature. They are the residue of the etching reagent ($FeCl_3$) or copper chloride. Hot soaking did not result in removal of dark spots in case of both sample after etching and sample after delamination – their presence is independent of the graphene separation method and they constitute contamination from the graphene production process.

Graphene after delamination lies down on the substrate better than graphene after etching and there are visible large flat areas between creases. Lower surface development is confirmed by the height unevenness profile along the line with length of 2 μm (marked red on Fig. 4). Between creases with average height fluctuating at about 5 nm, the surface is even and fluctuations in height of flat areas are within the range of 1 nm. The sample after chemical etching presents a completely different

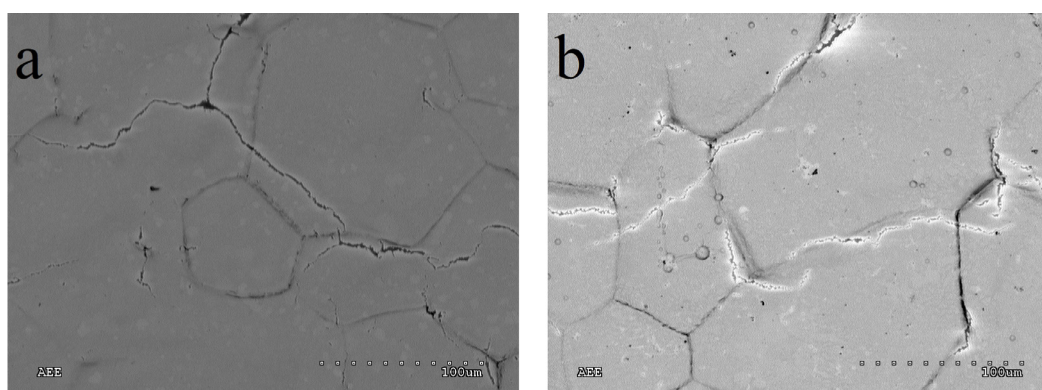

Fig. 2. Graphene on PMMA, a) after delamination, b) after etching in $FeCl_3$. SEM image, AEE mode

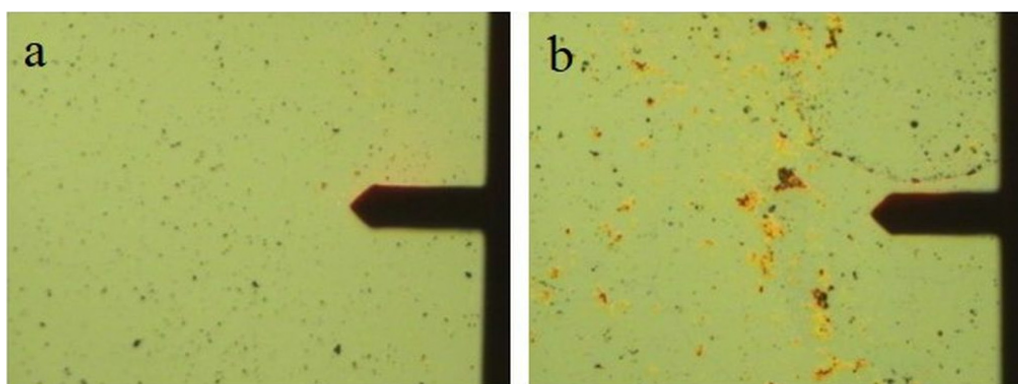

Fig. 3. Preview of graphene on an optical microscope compatible with the atomic force microscope a) after delamination, b) after chemical etching

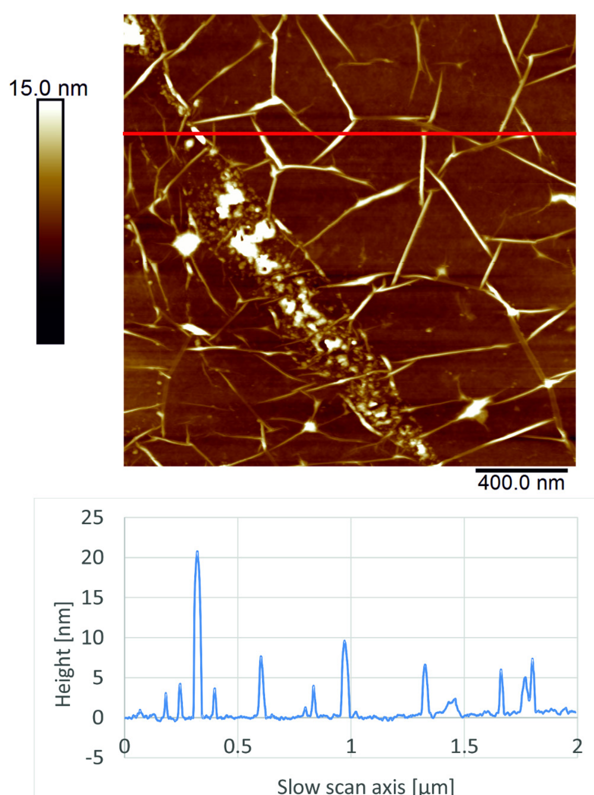

Fig. 4. AFM image and height profile (red line – scan axis) of graphene after delamination. Sample after hot soaking

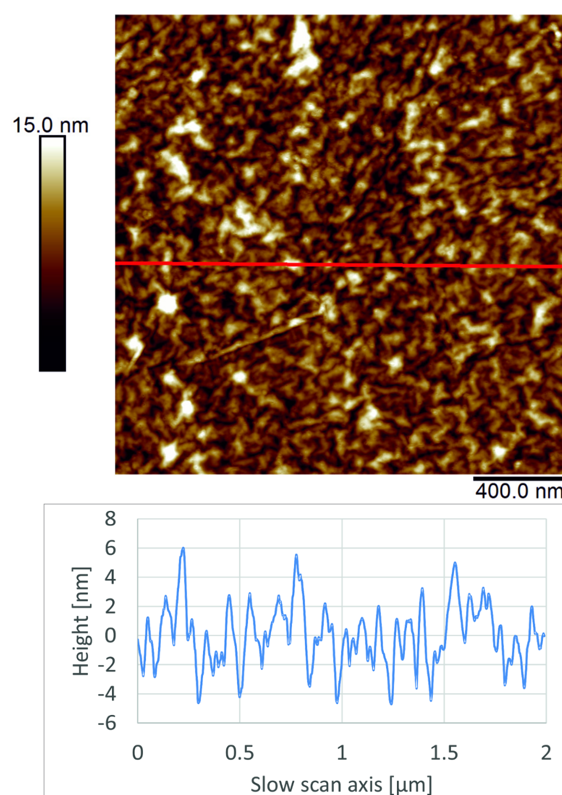

Fig. 5. AFM image and height profile (red line – scan axis) of graphene after chemical etching. Sample after hot soaking

height profile (Fig. 5), where the height amplitude is also within the range of 10 nm, but there do not occur any flat areas and it is difficult to indicate any specific creases like those present in graphene after delamination – the surface is more developed here. Aritmetical mean height (Sa) for delaminated graphene sample is 0.91 nm, for etched graphene Sa equals 1.90 nm. Similarly root mean square height (Sq) is 1.50 nm to 2.41 nm. Higher surface development in case of graphene after etching may indicate that the contact side of graphene, in this case being in contact with silicon oxide, is much purer after delamination. The side of graphene that adhered to the growth substrate, not the one onto which the polymer was applied, is laid on the target substrate during the transfer. Thus, it is the remains of copper, iron chloride, chlorine or copper chloride that determine impediment transfer to a new substrate. Contaminations are locations with tendency to retain e.g. water during the transfer, which is the cause behind creases and development of the surface. Graphene after delamination is on the opposite end of this spectrum since it is pure and therefore its surface is less developed, allowing us to notice smooth areas between creases.

3.3. Evaluation of graphene defectiveness degree by means of Raman spectroscopy

When analysing the Raman spectra of graphene (Fig. 6) separated from the growth substrate using the two methods concerned, it can be noticed that in case of graphene after

electrochemical delamination the ratio of intensity of peak G to intensity of peak D is almost two times lower than in case of graphene after chemical etching. The D band itself is less intensive after delamination, while the D' peak is more pronounced after etching. This indicates a lower number of defects after delamination. The half width of the 2D peak indicates defectiveness as well. When dealing with a monolayer without defects, the half width for 2D is 25-30 cm^{-1}. Graphene after delamination is very close to that value (31 cm^{-1}), while graphene after etching is characterised by greater half width of that peak (41 cm^{-1}). The presence of graphene monolayer is confirmed by symmetry of the 2D peak in both cases [26]. The quotient of 2D peak intensity and G peak intensity amounting to 3.94 is very close to the value of 4 present in the literature, which testifies to presence of a layer with thickness of a single atom. The lower quotient of intensity of these peaks for graphene after etching is caused by a greater amount of defects, not by the presence of the multilayer. The D+G peak occurs more clearly for the sample after etching, while for the delaminated sample it is practically imperceptible. The lack presence of this peak or very low intensity thereof indicate better structural arrangement. According to the relationship presented in the literature [27], the average calculated distance between defects for the etched sample is 15 nm, while for the sample after delamination it is 21 nm.

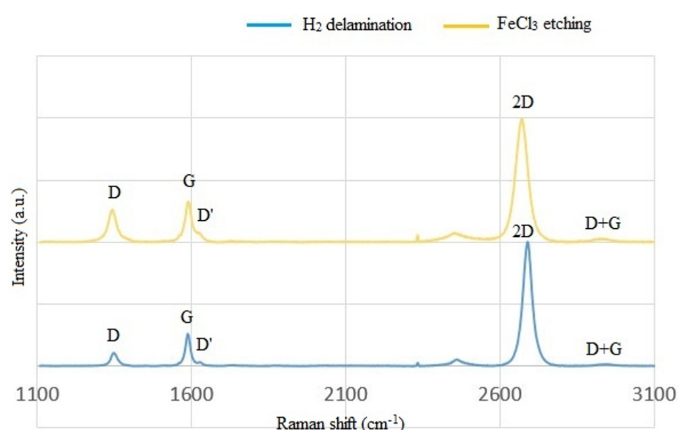

Fig. 6. Raman spectrum of graphene after chemical etching and after hydrogen delamination

3.4. Impact of graphene separation method on the degree of its contamination

An examination with the use of transmission electronic microscopy of samples separated by means of electrochemical delamination and chemical etching was performed in order to evaluate the degree of contamination of graphene surface.

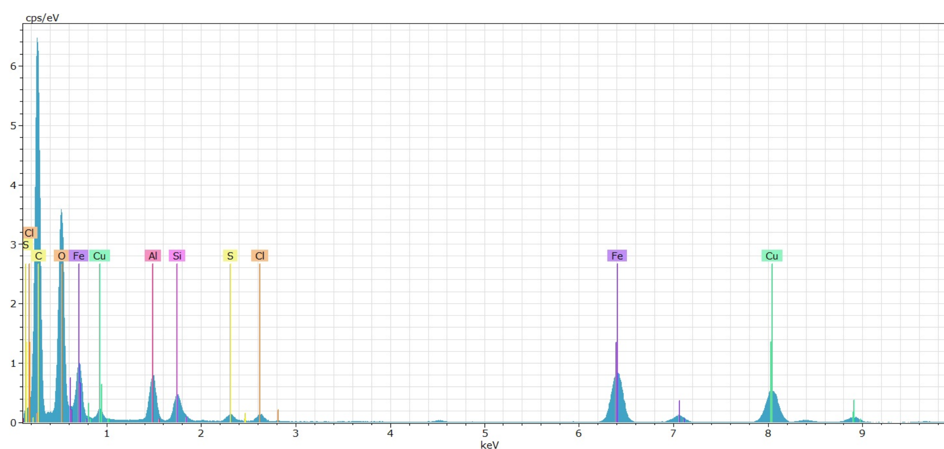

Fig. 7. Spectrum of elements in the graphene sample after chemical etching. EDS TEM analysis

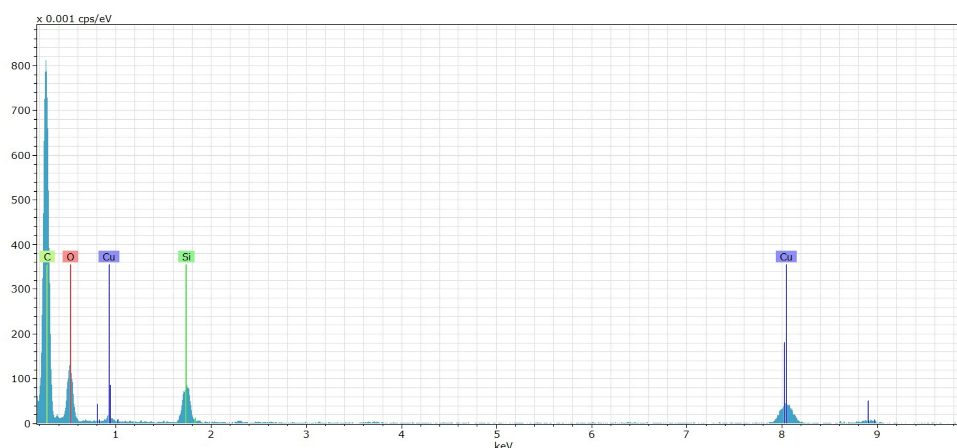

Fig. 8. Spectrum of elements in the graphene sample after electrochemical delamination. EDS TEM analysis

Examinations with the use of TEM microscope with EDS detector showed that graphene after chemical etching is contaminated to a major extent with iron and chlorine, which originate both from etching in the $FeCl_3$ solution and rinsing in the HCl solution after etching. The spectrum (Fig. 7) shows also peaks caused by copper. They are caused mainly by the substrate, since the mesh used for examinations, onto which graphene is deposited, is made of copper. Oxygen is also present and it is a sign of surface oxidation taking place. Other elements detected include sulphur, silicon and aluminium. Silicon comes most likely from graphene coming in contract with the laboratory glass, while the aluminium comes from the production process (ceramic parts of the furnace).

4 elements – copper, oxygen, silicon and carbon – were identified on the spectrum presenting the peaks from individual elements (Fig. 8) present in the sample after chemical delamination. The TEM mesh was also made of copper in that case. Similarly to the situation after chemical etching, the graphene after delamination includes oxygen coming from surface oxidation and silicon coming from the glass that the graphene came in contact with during subsequent phases of transfer. However, there is no chlorine or iron (coming from the reagent) and no aluminium, which remains on the growth substrate in this case.

4. Conclusions

Substituting separation of graphene by means of chemical etching with the electrochemical delamination method allows significant increase in rate of transfer of graphene layers without introducing any mechanical damage to the layer separated. Additionally, graphene separated using the delamination method is much purer, less defective at the atomic level and characterised by higher degree of structural arrangement. AFM examination showed that purity has a significant impact on the effect of graphene transfer onto smooth silicon substrates – the surface of graphene after transfer is even, with only a small number of creases. Separation by means of electrochemical delamination is a method that is much friendlier to the environment thanks to application of reagents that are less aggressive and easier to dispose of. This also provides a potential opportunity to reuse the growth substrate to produce graphene in subsequent procedures, which may result in reduced costs and faster production.

REFERENCES

[1] G.N. Dash, R. Pattanaik, R. Behera, J. Electron Devices Soc. **2** (5), 77-104 (2014).

[2] E. Pop, V. Varshney, A.K. Roy, MRS Bull. **37**, 1273-1281 (2012).

[3] L. Liao, Y.C. Lin, M. Bao, R. Cheng, J. Bai, Y. Liu, Y. Qu, K.L. Wang, Y. Huang, X. Duan, Nature **467**, 305-308 (2010).

[4] F. Zhang, J. Tang, N. Shinya, L. C. Qin, Chem. Phys. Lett. **584**, 124-129 (2013).

[5] Z. Wang, A. Wu, L.C. Ciacchi, G. Wei, Nanomaterials **8** (2), 65 (2018).

[6] A.K. Geim, K.S. Novoselov, Nature Materials **6**, 183-191 (2007).

[7] K.S. Novoselov, A.K. Geim, S.V. Morozov, D. Jiang, Y. Zhang, S.V. Dubonos, I.V. Grigorieva, A.A. Firsov, Science **306**, 666-669 (2004).

[8] C. Reeves, Graphene: Characterization after mechanical exfoliation, Senior, Physics, College of William and Mary (2010).

[9] Y.H. Wu, T. Yu, Z.X. Shen, Journal of Applied Physics **108**, 071301 (2010).

[10] G.R. Yazdi, T. Iakimov, R. Yakimova, Crystals **6** (5), 53 (2016).

[11] M. Aliofkhazraei, N. Ali, W.I. Milne, et al. Graphene science handbook. Fabricaion methods. CRC Press (2016).

[12] X. Li, C.W. Magnuson, A. Venugopal, R.M. Tromps, J.B. Hannon, E.M. Vogel, L. Colombo, R.S. Ruoff, J. Am. Chem. Soc. **133** (9), 2816-2819 (2011).

[13] A. Olsson, Graphene Growth through Chemical Vapor Deposition – Optimization of Growth and Transfer Parameters (2017).

[14] X. Li, W. Cai, L. Colombo, R.S. Ruoff, Nano Letters **9**, 4268-4272 (2009).

[15] P. Kula, R. Pietrasik, K. Dybowski, R. Atraszkiewicz, Ł. Kaczmarek, W. Szymański, P. Niedzielski, D. Nowak, W. Modrzyk, Nanotech **1**, 210-212 (2013).

[16] P. Kula, R. Pietrasik, K. Dybowski, R. Atraszkiewicz, W. Szymański, Ł. Kołodziejczyk, P. Niedzielski, D. Nowak, Appl. Mech. Mater. **510**, 8-12 (2014).

[17] Y. Ren, C. Zhu, W. Cai, H. Li, Y. Hao, Y. Wu, S. Chen, Q. Wu, R. D. Piner, S. Ruoof, Nano **7** (1), 1150001 (2012).

[18] J.W. Suk, A. Kitt, C.W. Magnusson, Y. Hao, S. Ahmed, J. An, A.K. Swan, B.B. Goldberg, R.S. Ruoff, ACS Nano **5** (9), 6916-6924 (2011).

[19] Y. Wang, Y. Zheng, X. Xu, E. Dubuisson, Bao, J. Lu, K.P. Loh, ACS Nano **5** (12), 9927-9933 (2011).

[20] T. Ciuk, I. Pasternak, A. Krajewska, J. Sobieski, P. Caban, J. Szmidt, W. Strupinski, J. Phys. Chem. C **117** (40), 20833-20837 (2013).

[21] C.T. Cherian, F. Giustiniano, I. Martin-Fernandez, H. Andersen, J. Balakrishnan, B. Özyilmaz, Small **11** (2), 189-194 (2015).

[22] A.I. Istrate, M. Veca, F. Nastase, A. Baracu, R. Gavrila, F. Comanescu, 2016 International Semiconductor Conference (CAS) (2016), DOI: 10.1109/SMICND.2016.7783071.

[23] L. Gao, W. Ren, H. Xu, L. Jin, Z. Wang, Teng Ma, L.P. Ma, Z. Zhang, Q. Fu, L. M. Peng, X. Bao, H.M. Cheng, Nat. Commun. **3** (2012), DOI: 10.1038/ncomms1702.

[24] C.J. Lockhart de la Rosa, J. Sun, N. Lindvall, M.T. Cole, Y. Nam, M. Löffler, E. Olsson, K.B. K. Teo, A. Yurgens, Appl. Phys. Lett. **102**, 022101 (2013).

[25] K. Verguts, J. Coroa, C. Huyghebaert, S. De Gendt, S. Brems, Nanoscale **10** (12), 5515-5521 (2018).

[26] M. Wall, Advanced Materials and Processes **170** (4), (2012).

[27] L.G. Cançado, A. Jorio, E.H. Martins Ferreira, F. Stavale, C.A. Achete, R.B. Capaz, M.V.O. Moutinho, A. Lombardo, T.S. Kulmala, A.C. Ferrari, Nano Lett. **11** (8), 3190-3196 (2011).